ISSN (Online) 2456-1290

International Journal of Engineering Research in Mechanical and Civil Engineering (IJERMCE)

Volume 11, Issue 8, August 2024

Investigation of Effects of Individual Gas Properties in Phase Change Property of Biogas

[1] Anilkumar Kosna, [2] Bade Shrestha

[1][2] Department of Mechanical and Aerospace Engineering, Western Michigan University, Kalamazoo, Michigan
Email: [1] anil.kumar@wmich.edu; [2] bade.shrestha@wmich.edu

***Abstract*— Biogas, increasingly utilized in recent years as a renewable energy source, is derived from the decomposition of organic materials such as manure, sewage sludge, or crop fodder in anaerobic digesters. Its primary components include methane (about 40 to 70%), carbon dioxide (CO2, approximately 15 to 60%), and trace amounts of other gases (around 1 to 3%). Typically, biogas is refined into bio-methane for commercial purposes by purifying it, a process involving the removal of carbon dioxide through various technologies like absorption, adsorption, permeation, and cryogenic methods. Among these, cryogenic technology stands out as a widely employed method, relying on the phase change properties of individual gases within the mixture.**

The paper investigated the impact of these phase change properties on biogas using a modified Peng-Robinson equation of state. The results successfully quantified the phase change characteristics of biogas, further validated through experiments conducted with three different biogas compositions: 50% carbon dioxide (CO2) - 50% methane (CH4), 80% CO2 - 20% CH4, and 100% CO2. The disparities between the results derived from the mixture's equation of state and the experimental findings ranged from 3.5% to 26.9%, a variance deemed acceptable considering experimental uncertainties.

***Index Terms*— Biogas, critical conditions of gases, vapor-liquid state, Peng-Robinson equation, renewable energy**

I. INTRODUCTION

Biogas plays a pivotal role in the renewable energy sector, particularly evident in the European Union (EU-28), where bioenergy, primarily driven by biogas, holds a substantial share of at least 25% as of 2020 according to Sun et al. [1]. The global landscape is poised for significant growth in commercial biogas capacity, projected to surge from 14.5 Gigawatts (GW) in 2012 to 29.5 GW by 2022 [1]. According to Global Bioenergy Statistics 2017, global biogas production reached 58.7 billion Nm3, with leading contributors being China (15.0 billion Nm3), the USA (8.48 billion Nm3), Thailand (1.30 billion Nm3), India (0.81 billion Nm3), Canada (0.79 billion Nm3), and the EU-28 (28.9 billion Nm3). The EU-28 nations dominate with a 49.8% production share, while Asia, America, and other continents contribute 31.9%, 16.7%, and 1.5%, respectively [2].

Biogas is generated in three main types of production plants: Industrial/commercial biogas plants (>300 m^3), farm scale/community biogas plants (100 – 250 m^3), and household/domestic biogas plants (1 – 12 m^3). While the composition of biogas varies based on the feedstock, it typically comprises methane (CH_4), carbon dioxide (CO_2), and small quantities of ammonia (NH_3), hydrogen sulfide (H_2S), hydrogen (H_2), oxygen (O_2), nitrogen (N_2), and carbon monoxide (CO). Commercialization of biogas involves its conversion into biomethane, a purified form achieved by removing carbon dioxide, hydrogen sulfide, and other gases through various purification processes. This purification enhances the lower heating value, compression capabilities, and reduces transportation costs. Biomethane shares properties with natural gas, making it suitable for distribution in natural gas grids, utilization as vehicle fuel, and efficient electricity production.

Various commercial purification technologies are available for processing biogas, including absorption, adsorption, permeation or membrane, and cryogenic methods. The absorption process can be further categorized into physical and chemical absorption. Physical absorption relies on the solubility of CO_2 and H_2S in an absorbent, typically water or polyethylene, while chemical absorption involves the formation of reversible chemical bonds between the solutes (CO_2 & H_2S) and solvents (aqueous solutions of mono, di, or tri ethanolamine, or aqueous solutions of sodium, potassium, and calcium hydroxide).

Adsorption, another purification method, is based on a material's ability to absorb CO_2 gas under pressure. Common materials for this process include molecular sieves like zeolite and active carbon. Permeation or membrane technology relies on the permeability properties of membranes for different gases. Lastly, cryogenic technology is centered on the de-sublimation of CO_2, functioning at high pressure (40 bars) and low temperatures (-100°C).

It's worth noting that these purification technologies require substantial investments and ongoing maintenance, making them more prevalent in large-scale plants such as industrial and farm-scale facilities. Unfortunately, there are currently no commercial purification technologies tailored for small-scale plants, specifically those designed for household use.

Household and small-scale biogas plants, typically ranging from 1 to 12 m^3 in capacity, are prevalent in developing countries of Asia, where supportive legislation and subsidies facilitate their installation. China and India lead in household

ISSN (Online) 2456-1290

International Journal of Engineering Research in Mechanical and Civil Engineering (IJERMCE)

Volume 11, Issue 8, August 2024

biogas production, accounting for nearly 80% of the total biogas plants. In India, there are 4.5 million such plants [3]. China has an ambitious plan to reach 80 million biogas plants by 2020, with already 40 million plants installed [4]. These household biogas units primarily cater to cooking and lighting needs, and in some cases, small combustion engines are employed locally due to the lack of technology for efficient biogas storage and transport to the market.

Addressing this challenge requires the development of a portable commercial purification and storage technology. Such technology could significantly benefit rural populations in developing and underdeveloped countries, fostering economic growth, self-employment, and energy independence through decentralized energy generation.

Among existing commercial purification technologies, the cryogenic method aligns with some requirements of a portable biogas purification system. However, its drawback lies in high energy consumption, necessitating efficient heat exchangers or condensers, which can complicate the system. To address this, the proposed system opts for the condensation of CO_2 instead of de-sublimation, relying on the critical point for condensation under specific conditions. Critical conditions for pure gases are well-documented, but such data for mixtures is not readily available. This paper aims to propose a methodology for predicting vapor-liquid equilibrium (VLE) of a mixture based on existing data for pure gases. This prediction of vapor-liquid equilibrium ultimately provides critical properties of the mixture, crucial for designing portable biogas purification processes.

II. METHODOLOGY TO DETERMINE THE CRITICAL PROPERTIES OF A MIXTURE

The prediction of vapor-liquid equilibrium (VLE) plays a crucial role in defining the critical properties of a substance. Various equations of state (EOS) models are available for pure components to facilitate the prediction of vapor-liquid equilibrium. Some of these models are outlined in Table 1.

Table 1. Various equations of state (EOS) models.

S.No.	Name	Equation of state
1.	Van der Waals (1976)	$P = \frac{RT}{V-b} - \frac{a}{V^2}$
2.	Redlich – Kwong (1949)	$P = \frac{RT}{V-b} - \frac{a}{V(V+b)T^{0.5}}$
3.	Soave – Redlich – Kwong (1972)	$P = \frac{RT}{V-b} - \frac{a(T)}{V(V+b)}$
4.	Peng – Robinson (1976)	$P = \frac{RT}{V-b} - \frac{a(T)}{V(V+b)+b(V-b)}$
5.	Stryjek – Vera – Peng – Robinson (1986)	$P = \frac{RT}{V-b} - \frac{a(\theta,T)}{V(V+b)+b(V-b)}$
6.	Patel – Teja (1982)	$P = \frac{RT}{V-b} - \frac{a(T)}{V(V+b)+c(V-b)}$

Indeed, a typical equation of state consists of two terms, with the first term representing intermolecular interactions of repulsive force, and the second term accounting for attractive forces. The equation of state relies on the critical properties of a pure substance and includes empirical constants.

The Van der Waals equation of state stands as the simplest and oldest among all equations of states. This equation establishes a relationship between pressure (P), temperature (T), specific volume (V), and ideal gas constants (R) through empirical constants a, b, and m. These constants can be computed using critical pressure (Pc), critical temperature (Tc), acentric factor (ω), and an ideal gas constant (R).

In 1949, Redlich-Kwong observed that the Van der Waals equation is often inaccurate in predicting vapor-liquid equilibrium. They modified the equation by introducing temperature dependence to the attraction term. Later, in 1972, Soave replaced the temperature-dependent term with a more generalized temperature term, denoted as a(T), where:

$$a(T) = 0.4274 \left(\frac{R^2 {T_c}^2}{P_c}\right)\left(1 + m\left(1 - \left(\frac{T}{T_C}\right)^{0.5}\right)\right)^2$$

$$m = 0.480 + 1.57\,\omega - 0.176\,\omega^2$$

$$b = 0.08664\,\frac{RT_C}{P_C}$$

In 1976, Peng-Robinson introduced a redefinition of the constant a(T) from the Soave-Redlich-Kwong equation. The Peng-Robinson equation of state has emerged as the most popular and widely utilized method for predicting vapor-liquid equilibrium [5]. The Peng-Robinson (1976) equation for a pure substance can be expressed as:

$$P = \frac{RT}{V-b} - \frac{a(T)}{V(V+b)+b(V-b)}$$

Where;

$$a(T) = 0.45724\,\frac{R^2 {T_c}^2}{P_c}\,(1 + k(1 - \left(\frac{T}{T_c}\right)^{0.5})^2$$

$$k = 0.37464 + 1.5422\,\omega - 0.26922\,\omega^2$$

$$b = 0.07780\,\frac{RT_C}{P_c}$$

Figures 1 and 2 depict the P-V (pressure-volume) diagram of pure CO_2 and CH_4, respectively, generated from the Peng-Robinson equation of state. These diagrams display various isotherms, representing different temperatures, allowing for the study of phase transformations of substances.

At critical pressure, an isotherm exhibits a slope of zero. The temperature and specific volume at this critical pressure are referred to as the critical temperature and critical specific volume, respectively. This critical point serves as a distinguishing marker between phases. At this point, the liquid and vapor phases coexist in equilibrium. The coexistence of vapor-liquid equilibrium is illustrated by the spinodal curve.

The spinodal curve provides insights into the fluid's

ISSN (Online) 2456-1290

International Journal of Engineering Research in Mechanical and Civil Engineering (IJERMCE)

Volume 11, Issue 8, August 2024

behavior in its saturation liquid state (left part of the curve) and saturated vapor state (right part of the curve). The critical point delineates the boundary between the saturated liquid and vapor phases. The region above and to the right of the spinodal curve denotes the superheated vapor region, while the left side represents the compressed liquid region. The area beneath the spinodal curve signifies the saturated vapor-liquid region.

The critical points obtained from the Peng-Robinson equation of state closely align with tabulated critical points, exhibiting less than 1% error, indicating the reliability and accuracy of the model.

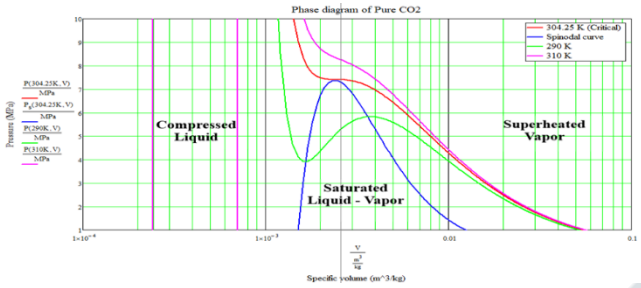

Figure 1. P-V diagram of Pure CO_2.

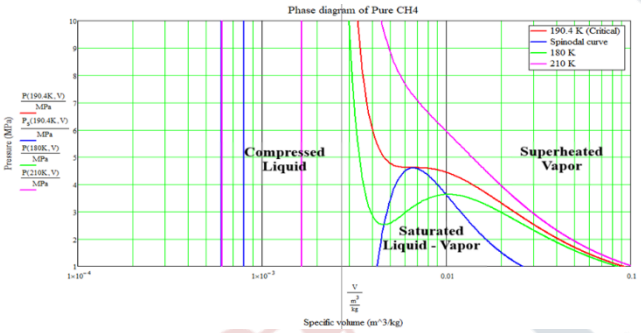

Figure 2. P-V diagram of Pure CH_4.

The Peng-Robinson equation of state for a pure substance can be extended to gas mixtures by employing appropriate mixing rules. Among these rules, Van der Waals mixing rules are commonly utilized in process simulations. Seif-Eddeen K. Fatten et al. [5] introduced a methodology for applying Van der Waals mixing rules to the Peng-Robinson equation of state for pure gases. In their study, they proposed a semi-empirical correlation for binary interaction parameters of the CH_4-CO_2 mixture to minimize the deviation of vapor-liquid equilibrium (VLE) predictions from experimental data. The equations used to develop the equation of state for the CO_2-CH_4 binary mixture are as follows:

$$P = \frac{R\ T}{(V - b_m)} - \frac{a_m(T)}{V\ (V + b_m) + b(V - b_m)}$$

The attraction parameter $a_m(T)$ can be expressed as,

$$a_m(T) = \sum_{i=1}^{2}\sum_{j=1}^{2} x_i x_j\ (1 - k_{ij})\sqrt{a_i a_j}$$

The repulsion parameter b_m as,

$$b_m = \sum_{i=1}^{2} x_i b_i$$

Binary interaction parameter k_{ij} can be written as,

$$k_{ij} = \frac{1}{2}\frac{b_j}{b_i}\sqrt{\frac{a_i}{a_j}} - \frac{1}{2}\frac{b_i}{b_j}\sqrt{\frac{a_j}{a_i}} + \frac{1}{2}\frac{b_j RT}{\sqrt{a_i a_j}}\frac{\theta_1}{(\frac{T}{T_{c,i}})^{\theta_2}}$$

Where;

x is a mole fraction.

a, and b are the attraction and repulsion terms of pure components.

$\theta_1 = 2.5522$, and $\theta_2 = 0.80726$ are the empirical constantans of the methane/carbon dioxide mixture [5]

Figure 3 displays the P-V (pressure-volume) diagram of the 50% CO_2 – 50% CH_4 binary mixture obtained from the modified Peng-Robinson equation of state. The critical states of the CO_2 – CH_4 mixture are identified at 255 K (-18 ºC), 4.82 MPa (699.08 psia), and 0.0045 m^3/kg. This representation clarifies that, for the specified mixture, the vapor-liquid equilibrium of CO_2 coexists at the critical point, providing insight into the critical conditions and behavior of the mixture under these parameters.

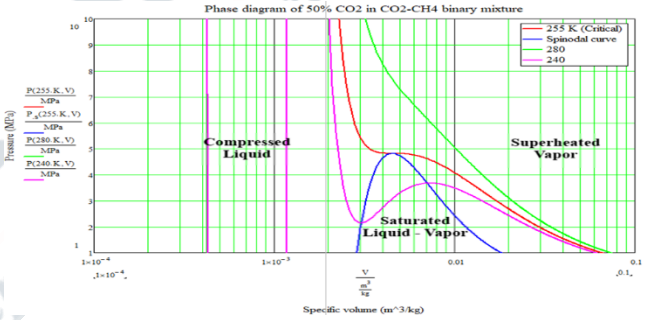

Figure 3. P-V diagram of 50% CH_4 – 50% CO_2.

Figures 4, 5, and 6 depict the critical temperature, pressure, and specific volume as functions of CO_2 composition, as derived from the equation of state for the CO_2 – CH_4 mixture. These figures provide a visual representation of how these critical properties vary with different proportions of CO_2 in the mixture.

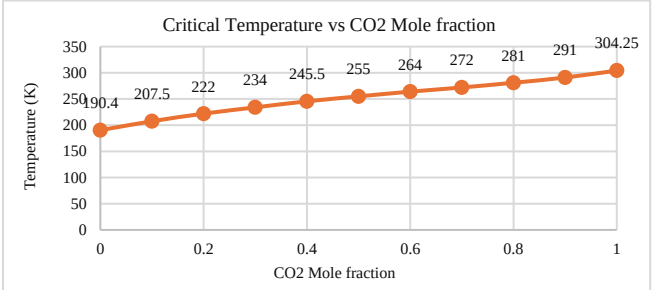

Figure 4. Critical Temperature against CO_2 Mole fraction

ISSN (Online) 2456-1290

International Journal of Engineering Research in Mechanical and Civil Engineering (IJERMCE)

Volume 11, Issue 8, August 2024

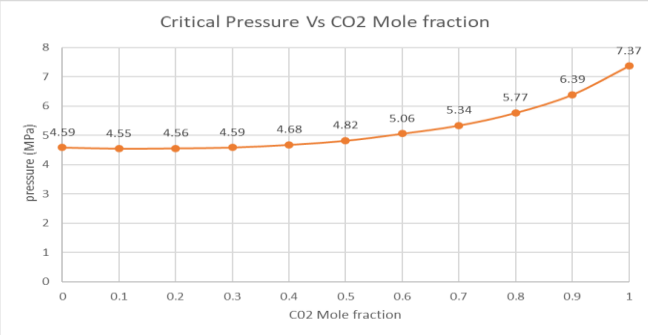

Figure 5. Critical Pressure against CO_2 Mole fraction

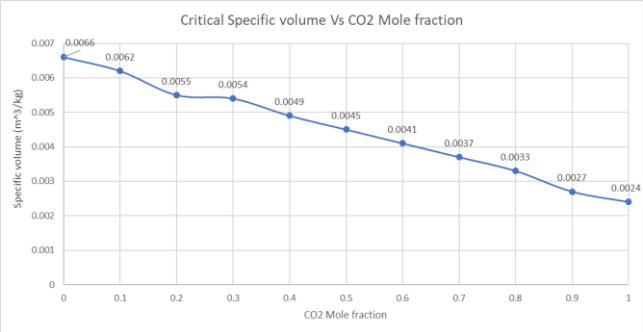

Figure 6. Critical Specific volume against CO_2 Mole fraction

III. EXPERIMENTAL SETUP

The proposed equation of state for a mixture of CO_2 – CH_4 has successfully identified the critical states of variable compositions within the CO_2 – CH_4 binary mixture. To validate the equation of state for biogas, an experiment has been devised. The typical equation of state establishes the relationship between the state variables—pressure (P), temperature (T), and specific volume (v). In a closed system, the variation of pressure and temperature is independent of the specific volume, simplifying the variables to pressure and temperature.

The experimental setup involves a closed system where pressure and temperature are recorded at a constant specific volume. This data on pressure and temperature can then be employed to validate the equation of state for the mixture by comparing the theoretical and experimental pressure and temperature data. A schematic representation of the experimental layout is illustrated in Figure 7.

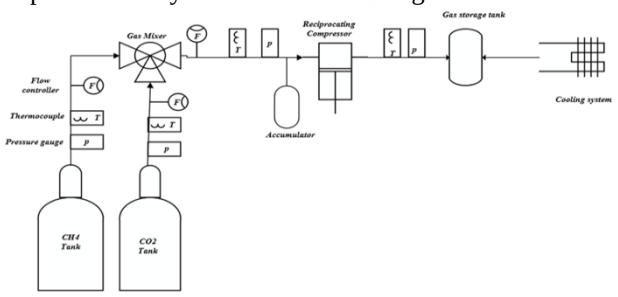

Figure 7. Experimental setup

The procedure for the experiment involved opening the valves of pure gas tanks containing CH_4 and CO_2 to achieve the desired pressure and flow rate within the gas mixing system. After releasing the pure gases into the system, the flow meters were manually adjusted to specified flow rates based on the required volume fractions of the binary mixture. Subsequently, the binary mixture from the gas mixing system was directed to an accumulator to establish the inlet pressure for the compressor. The operation of this accumulator was regulated using a needle valve to control the flow of the binary mixture to the compressor.

The compressor was configured to operate at the gas storage tank's predetermined pressure. Upon activating the compressor, it was left running for 4 to 5 seconds to build suction pressure. Following this, the valve of the accumulator was opened to allow the binary mixture into the compressor inlet. Once the gas storage tank reached the adjusted pressure, the compressor automatically shut off. Throughout the process, variations in pressure and temperature at different locations were recorded for analysis and validation of the experimental data.

The experiment was conducted for three different gas compositions: Pure CO_2, 80% CO_2 – 20% CH_4, and 50% CO_2 – 50% CH_4. The specific inputs needed for the gas mixing equipment corresponding to each composition are detailed in Table 2.

Table 2. Inputs of gas mixing equipment.

S.no.	X_{CO2}	X_{CH4}	$Vdot_{CO2}$ $(\frac{m^3}{hr})$	$Vdot_{CH4}$ $(\frac{m^3}{hr})$	$Vdot_{mixture}$ $(\frac{m^3}{hr})$
1.	1	0	1.98	0	1.98
2.	0.8	0.2	1.58	0.39	1.98
3.	0.5	0.5	0.99	0.99	1.98

IV. VALIDATION OF EQUATION OF STATE

The validation of the equation of state for the CO_2 – CH_4 binary mixture was accomplished by comparing the theoretical and experimental saturated vapor pressure and temperature at constant specific volume. As outlined in the experimental procedure, all mixtures were compressed to 12.4 MPa (the operating pressure of the gas storage tank) and subsequently cooled to the saturated vapor temperature (determined from the equation of state) to experimentally

ISSN (Online) 2456-1290

International Journal of Engineering Research in Mechanical and Civil Engineering (IJERMCE)

Volume 11, Issue 8, August 2024

determine the saturated vapor pressure at a constant volume. This comparison allowed for the assessment of the equation of state's accuracy and reliability in predicting the behavior of the $CO_2 – CH_4$ mixture under specified conditions.

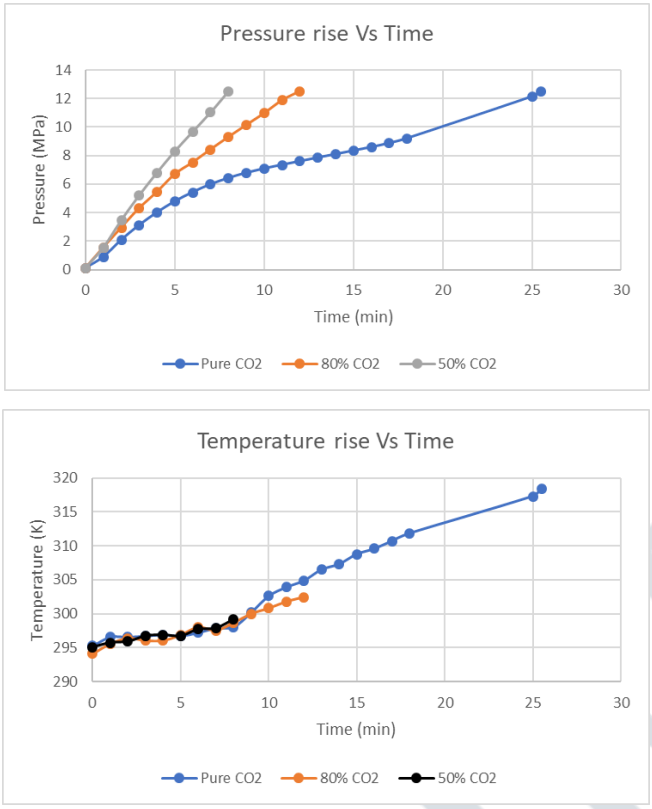

Figure 8. Pressure & Temperature rise vs Time

Figure 8 illustrates the pressure and temperature increase of various binary mixtures during the compression process. It highlights the interdependence of pressure and temperature, showcasing that as pressure rises, so does temperature, and vice versa. The compression time of gases varied depending on their composition, with pure CO_2, 80% CO_2 – 20% CH_4, and 50% CO_2 – 50% CH_4 having compression times of 25.5 minutes, 12 minutes, and 8 minutes, respectively. This variation in compression time indicates that heavier molecules require more energy for compression.

Despite all mixtures being stored in the same tank at the same pressure, the mass of fluid stored differed due to the varying molecular weights of the mixtures. Once the compression was completed, the valve of the gas storage tank was closed, rendering it a closed system. The properties of the gas mixture after compression are detailed in Table 3.

Table 3. Properties of fluid after compression

Mixture	$m_{mixture}$ (kg)	m_{CO2} (kg)	m_{ch4} (kg)	$v_{mixture}$ $(\frac{m^3}{kg})$	P (MPa)	T (K)
Pure CO_2	--------	0.532	--------	2.846×10^{-3}	12.49	318.41
80% CO_2	0.280	0.257	0.023	5.403×10^{-3}	12.50	302.43
50% CO_2	0.173	0.127	0.046	8.761×10^{-3}	12.51	299.17

The saturated vapor properties of the mixture at a specified specific volume, obtained from the equation of state, are presented in Table 4. Once the saturated vapor temperatures were determined, the next step involved maintaining the saturated vapor temperature to record the experimental saturated vapor pressure of the mixture. The experimental saturated vapor pressure was then compared to the theoretical saturated vapor pressure to validate the equation of state.

For pure CO_2, the required saturation temperature is 301 K, which is higher than the ambient air temperature (295 K). Therefore, natural convection of ambient air was sufficient to dissipate heat from the storage tank. On the other hand, the mixture's saturated vapor temperature is lower than the ambient temperature, and natural convection alone cannot achieve the required temperature drop. Hence, external cooling (provided by dry ice) was employed to reach the necessary low saturated vapor temperature. Dry ice, the solid form of CO_2, sublimates at 194.65 K (-78.5 ℃) under atmospheric pressure. By covering the gas storage tank with dry ice, the sublimation process cooled the tank to around 218 K (-55 ℃), effectively cooling the gas mixture to the required temperature.

Figure 9 shows the pressure drop for the three different gas compositions during cooling. The pressure of mixture at saturated vapor temperature was recorded and later compared to theoretical saturated vapor pressure for validation of the proposed equation of state. The error percentage of the validation was calculated as:

$$Error\ \% = \left| \frac{P_{exp} - P_{the}}{P_{exp}} * 100 \right|$$

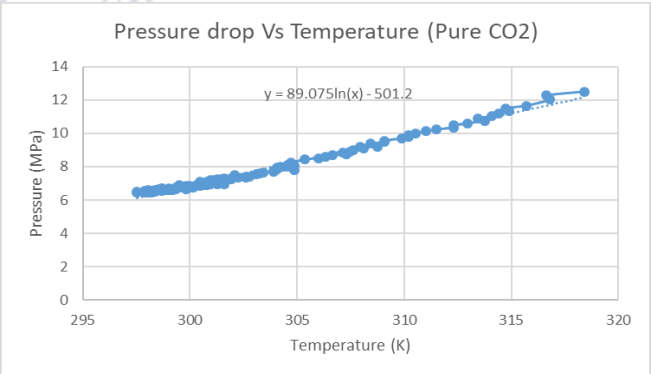

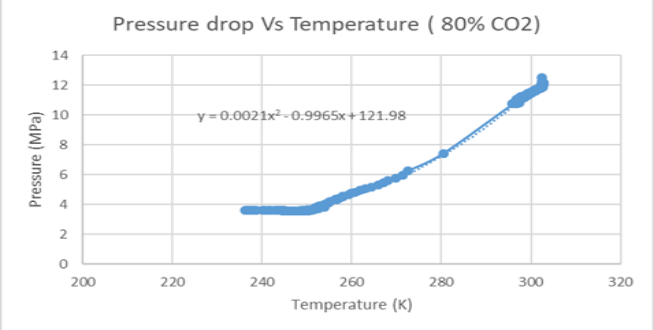

ISSN (Online) 2456-1290

International Journal of Engineering Research in Mechanical and Civil Engineering (IJERMCE)

Volume 11, Issue 8, August 2024

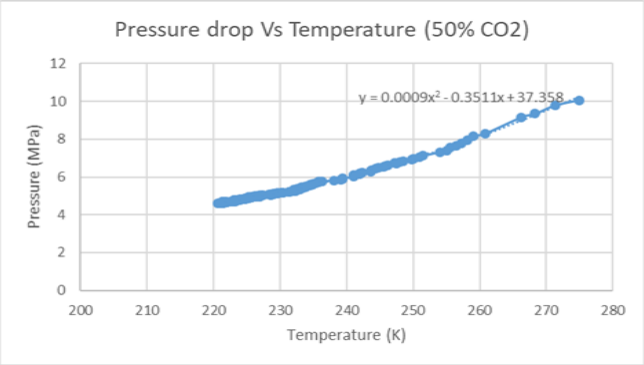

Figure 9. Experimental pressure drops vs Temperature.

Table 4 shows the comparison of experimental saturated vapor pressure with the theoretical vapor pressure at saturated vapor temperature. The difference between the theoretical values and the experimental results were comparable and the error has increased as the composition has more methane.

Table 4. Comparison of theoretical and experimental saturated vapor pressure.

Mixture	$T_{saturated}$	$P_{saturated}$ (theoretical)	$P_{saturated}$ (Experimental)	Error %
Pure CO_2	301 K	6.91 MPa	7.16 MPa	3.49
80% CO_2	261 K	3.96 MPa	4.94 MPa	19.83
50% CO_2	224 K	2.83 MPa	3.87 MPa	26.63

V. CONCLUSION

This paper has successfully investigated the impact of critical conditions of individual gases on gas mixtures, providing a quantitative analysis of the critical properties for various compositions of biogas. The experimental saturated pressure of pure CO_2 closely aligned with the theoretically calculated saturated pressure, yielding a minimal error percentage of 3.49%. However, for mixtures such as 80% CO_2 – 20% CH_4 and 50% CO_2 – 50% CH_4, the error percentages were higher at 19.83% and 26.63%, respectively. This elevated error in mixtures primarily resulted from the lower saturated temperature and the cooling system employed in the experiment.

The findings highlight the potential application of the simulation model in determining the vapor-liquid states of biogas, particularly in the design of biogas purification processes. The insights gained from this study could contribute to the development of more efficient and accurate methods for designing systems that purify biogas for various applications.

ACKNOWLEDGEMENT

The support of the Department of Mechanical and Aerospace Engineering, Western Michigan University to this research is acknowledged.

REFERENCES

[1] Q. Sun, H. Li, J. Yan, L. Liu, Z. Yu, and X. Yu, “Selection of appropriate biogas upgrading technology-a review of biogas cleaning, upgrading and utilization,” Renew. Sustain. Energy Rev., vol. 51, no. January, pp. 521–532, 2015.

[2] Bharadwaj Kummamuru, “Wba Global Bioenergy Statistics 2017,” p. 80, 2017.

[3] R. M. Kapoor and V. K. Vijay, “Evaluation of Existing Low Cost Gas Bottling Systems for Vehicles Use Adaption in Developing Economies,” p. 59, 2013.

[4] K. Rajendran, S. Aslanzadeh, and M. J. Taherzadeh, Household biogas digesters-A review, vol. 5, no. 8. 2012.

[5] S. K. Fateen, M. M. Khalil, and A. O. Elnabawy, “Semi-empirical correlation for binary interaction parameters of the Peng – Robinson equation of state with the van der Waals mixing rules for the prediction of high-pressure vapor – liquid equilibrium,” pp. 137–145, 2013.